Thermodynamics of the two-dimensional *XY* model from functional renormalization

P. Jakubczyk[1,2,*] and A. Eberlein[3,†]

[1]*Institute of Theoretical Physics, Faculty of Physics, University of Warsaw, Pasteura 5, 02-093 Warsaw, Poland*

[2]*Max Planck Institute for Solid State Research, Heisenbergstrasse 1, 70569, Stuttgart, Germany*

[3]*Department of Physics, Harvard University, Cambridge, Massachusetts 02138, USA*

(Received 21 April 2016; published 29 June 2016)

We solve the nonperturbative renormalization-group flow equations for the two-dimensional *XY* model at the truncation level of the (complete) second-order derivative expansion. We compute the thermodynamic properties in the high-temperature phase and compare the nonuniversal features specific to the *XY* model with results from Monte Carlo simulations. In particular, we study the position and magnitude of the specific-heat peak as a function of temperature. The obtained results compare well with Monte Carlo simulations. We additionally gauge the accuracy of simplified nonperturbative renormalization-group treatments relying on ϕ^4-type truncations. Our computation indicates that such an approximation is insufficient in the high-T phase and a correct analysis of the specific-heat profile requires account of an infinite number of interaction vertices.

DOI: 10.1103/PhysRevE.93.062145

I. INTRODUCTION

It has long been recognized [1–5] that the two-dimensional *XY* model undergoes a Kosterlitz-Thouless (KT) phase transition upon varying temperature T. This transition is peculiar in a number of respects: it is not accompanied by the appearance of long-range order (which is prohibited by the Mermin-Wagner theorem [6]) and the free energy is a smooth (C^∞ class) function of the thermodynamic parameters. Nonetheless, the low-T phase displays long-range correlations and order-parameter stiffness. The latter exhibits a universal jump upon crossing the transition temperature T_{KT}. The correlation length is characterized by an essential singularity in the vicinity of the transition in the high-T phase. A distinct nonuniversal feature of the *XY* model is the pronounced, asymmetric peak of the specific heat as a function of T. The occurrence of this maximum is usually attributed to a rapid increase of entropy upon unbinding the vortex-antivortex pairs. The peak is located somewhat above the transition temperature T_{KT}. It is peculiar that, on the one hand, the maximum is well separated from the asymptotic critical region, and, on the other hand, it occurs in a temperature range where the correlation length is still very large compared to the microscopic scale.

The Kosterlitz-Thouless transition is relevant in a number of physical contexts [7] such as magnetism, liquid crystals, melting of two-dimensional ($d = 2$) solids, superfluidity, and superconductivity. Experimentally the KT-type behavior was observed in liquid-helium films [8–10] and atomic gases [11–14].

The universal aspects of the KT transition are conventionally described in the language of vortex-antivortex pair unbinding and a mapping to a Coulomb gas or sine-Gordon field theory. The predictivity of such formulations is typically restricted to the behavior in the vicinity of the transition, which makes it harder to access the nonuniversal, system-specific properties, such as the critical temperature or the position, magnitude, and width of the specific-heat peak.

In the present work, we develop and extend the description of the KT transition using the nonperturbative renormalization group (RG). We build upon earlier works [15–17], which, however, were limited to ϕ^4-type effective models and focused exclusively on universal aspects of the transition. The formulation evades the explicit introduction of vortices as degrees of freedom, and, in the form presented here, takes a microscopic spin system as the starting point. On the other hand, the approach captures the long-wavelength infrared (IR) asymptotics and respects the Mermin-Wagner theorem. In the present analysis, we focus primarily on the relatively simple *XY* model on a square lattice, where the results obtained at different approximation levels of the RG framework can be compared to ample Monte Carlo (MC) data [18–25]. Observe, however, that the verification of the theoretical predictions of the KT theory by MC simulations has not always been conclusive, even with respect to the most basic properties. For a critical discussion of these issues, see Ref. [22]. The present approach complements the MC in that it is formulated directly for infinite volume and does not invoke finite-size scaling theory. It also differs from the standard RG treatments in evading the introduction of vortices or any expansions in powers of the order-parameter field. We show that the latter is crucial for a correct (even qualitatively) account of thermodynamics in the high-T phase. This is because temperature dependencies reside in all the interaction vertices and dropping some of them significantly deforms the results for the thermodynamic derivatives. In addition, in the vicinity of the transition, by standard power counting, all of the interaction vertices are relevant.

The nonperturbative RG is among the methods allowing for accurate computations of critical behavior in diverse systems. Its applicability, in addition, is by no means restricted to the vicinity of a phase transition. It has proven useful in a wide range of complex physical contexts. Examples include models with competing orders [26–29] or situations out of equilibrium [30–32]. The formalism by itself sheds light on fundamental aspects of critical phenomena (see, e.g., [33,34]), leading to a genuine progress of the field. On the other hand, seldom do the computations within this approach reach high-precision accuracy away from the critical region. The

*pawel.jakubczyk@fuw.edu.pl

†eberlein@physics.harvard.edu

precise predictions also typically depend somewhat on the choice of regularization. Reference [35] shows that the critical temperature of the three-dimensional Ising model may be calculated with an accuracy of around 1%. Going beyond this precision level would require a substantial effort. The presently analyzed case of the two-dimensional XY model is methodologically very distinct for at least two reasons: (1) The physics governing the vicinity of the phase transition is dominated by the anomalous dimension (which is negligible in $d = 3$ for most purposes); (2) fluctuation effects are stronger (and lead to the ultimate obliteration of long-range order) due to the presence of the Goldstone mode.

Our framework automatically encodes [36] the Mermin-Wagner theorem and is (upon slight modifications) extendable to more complex systems characterized by similar low-energy behavior at finite temperatures. These include quantum spins as well as interacting bosons or fermions in $d = 2$. Such systems were already studied within simpler nonperturbative RG truncations; see, e.g., [37–42]. However, the latter are not sufficient to correctly account for nonuniversal features related to the KT transition—see Sec. V. Before embarking on the more complex problems mentioned above, it is important to understand the merits and limitations of the method in situations where the results can be reliably compared to other approaches.

II. THE XY MODEL AND THE CORRESPONDING LATTICE FIELD THEORY

The classical XY model on a lattice is defined by the Hamiltonian

$$\mathcal{H}\big(\{\vec{s}_i\}_{i=1}^N\big) = -\tfrac{1}{2} J_{ij}\vec{s}_i\vec{s}_j, \tag{1}$$

where $i,j \in \{1,\dots,N\}$ label the sites of the lattice, $\vec{s}_i \in \mathbb{R}^2$, $|\vec{s}_i| = 1$, and the summation is implicit wherever the index appears exactly twice in a product expression.

The corresponding partition function is given by

$$\mathcal{Z} = \sum_{\{\vec{s}\}} e^{-\beta\mathcal{H}}, \quad \text{where} \quad \sum_{\{\vec{s}\}} = \int \prod_i d\theta_i. \tag{2}$$

Here, $\beta^{-1} = k_B T$ and θ_i denotes the angle between the vector $\vec{s}_i$ and the x axis, so that $\vec{s}_i\vec{s}_j = \cos(\theta_i - \theta_j)$ and $\theta_i \in [0, 2\pi[$ for each i.

In order to cast the problem of evaluating the partition function in the language of field theory, we employ the identity

$$e^{\frac{1}{2}A_{ij}\vec{s}_i\vec{s}_j} = \mathcal{N}^{-1}\int \prod_i d\vec{\psi}_i e^{-\frac{1}{2}(\mathbb{A}^{-1})_{ij}\vec{\psi}_i\vec{\psi}_j + \vec{s}_i\vec{\psi}_i}, \tag{3}$$

where the normalization factor is given by

$$\mathcal{N} = (2\pi)^N \det\mathbb{A}. \tag{4}$$

Here, $\vec{\psi}_i$ is a two-dimensional vector attributed to the lattice site i. Equation (3) applies provided the matrix $\mathbb{A}$ is positive definite. The nonpositivity can be cured by shifting the matrix by a constant diagonal term, which, in our setup, amounts to transforming the Hamiltonian given by Eq. (1) via

$$\mathcal{H}\big(\{\vec{s}_i\}_{i=1}^N\big) \longrightarrow \mathcal{H}_c\big(\{\vec{s}_i\}_{i=1}^N\big) = -\tfrac{1}{2} J_{ij}\vec{s}_i\vec{s}_j - \tfrac{1}{2} c\vec{s}_i\vec{s}_i, \tag{5}$$

i.e., shifting it by a constant equal to $\frac{1}{2}Nc$. Specifying

$$A_{ij} = \beta(J_{ij} + c\delta_{ij}), \tag{6}$$

we apply Eq. (3) to Eq. (2). The resulting expression for the partition function $\mathcal{Z}$ still involves the multiple integration over the spin variables ($\{\vec{s}\}$), which can now be explicitly performed,

$$\sum_{\{\vec{s}\}} e^{\vec{s}_i\vec{\psi}_i} = (2\pi)^N \prod_i I_0(|\vec{\psi}_i|). \tag{7}$$

Here, $I_\alpha(x)$ denotes the hyperbolic Bessel function of the first kind. In this way, we cast the partition function in the form

$$\mathcal{Z} = (\det\mathbb{A})^{-1}\int \prod_i e^{-\frac{1}{2}\vec{\psi}_i(\mathbb{A}^{-1})_{ij}\vec{\psi}_j + \sum_i \ln I_0(|\vec{\psi}_i|)}. \tag{8}$$

In order to make all of the temperature dependencies explicit, we rescale the interaction matrix $\mathbb{A}$ and the fluctuating field $\vec{\psi}$ according to

$$\tilde{A}_{ij} = \beta^{-1}A_{ij}, \quad \vec{\phi}_i = \beta^{-\frac{1}{2}}\vec{\psi}_i. \tag{9}$$

In this way, the partition function becomes expressed as

$$\mathcal{Z} = \int \mathcal{D}\vec{\phi} e^{-\beta S[\vec{\phi}]}, \tag{10}$$

with

$$\beta S[\vec{\phi}] = \frac{1}{2}\vec{\phi}_i(\tilde{\mathbb{A}}^{-1})_{ij}\vec{\phi}_j - \sum_i \ln I_0(\beta^{\frac{1}{2}}|\vec{\phi}_i|) \tag{11}$$

and

$$\mathcal{D}\vec{\phi} = (\det\tilde{A})^{-1}\prod_i d\vec{\phi}_i. \tag{12}$$

Importantly, the change of variables of Eq. (9) removes temperature dependencies from the integration measure $\mathcal{D}\vec{\phi}$ as well as the kinetic term $\frac{1}{2}\vec{\phi}_i(\mathbb{A}^{-1})_{ij}\vec{\phi}_j$ in the effective action $S[\vec{\phi}]$, and absorbs it fully into the local potential term $\ln I_0(\beta^{\frac{1}{2}}|\vec{\phi}_i|)$. This aspect is crucial for the validity of the subsequent approximate RG procedure of Secs. III and IV. The choice introduced in Eq. (9) differs from some standard conventions [43].

Equations (10)–(12) define the starting point for our computations. Specific lattice and interaction types may now be addressed by specifying the corresponding matrix $\mathbb{J}$. Assuming translational invariance, the kinetic term in $S[\vec{\phi}]$ is diagonalized with the Fourier transform:

$$\frac{1}{2}\vec{\phi}_i(\tilde{\mathbb{A}}^{-1})_{ij}\vec{\phi}_j = \frac{1}{2}\sum_{\vec{q}} \tilde{A}_{\vec{q}}^{-1}\vec{\phi}_{\vec{q}}\vec{\phi}_{-\vec{q}}, \tag{13}$$

where

$$\tilde{A}_{\vec{q}} = c + J_{\vec{q}} = c + \frac{1}{N}J_{ij}e^{i\vec{q}(\vec{r}_i - \vec{r}_j)}. \tag{14}$$

This establishes the explicit form of the kinetic term.

A. Mean-field theory for ferromagnetic order

Assuming a form of $\mathbb{J}$ favoring ferromagnetic ordering, one identifies the mean-field free energy as the minimum of

$S[\vec{\phi}]$. Restricting to uniform field configurations, the mean-field equilibrium value of $|\phi|$ is given by

$$\tilde{A}_0^{-1}|\vec{\phi}| - \frac{I_1(\beta^{1/2}|\vec{\phi}|)}{I_0(\beta^{1/2}|\vec{\phi}|)}\beta^{1/2} = 0. \tag{15}$$

The mean-field critical temperature is obtained by expanding the above around $|\vec{\phi}| = 0$ up to terms linear in $|\vec{\phi}|$. This relates the critical temperature to $\tilde{A}_0$:

$$k_B T_c = \tfrac{1}{2}\tilde{A}_0. \tag{16}$$

The corresponding critical exponents are classical and the critical temperature of Eq. (16) carries a strong, linear dependence on the parameter c [43]. Obviously, the resulting occurrence of long-range order at mean-field level contradicts the Mermin-Wagner theorem.

B. Nearest-neighbor interactions

For the square lattice with nearest-neighbor interactions, we obtain

$$J_{\vec{q}} = 2J[\cos(aq_x) + \cos(aq_y)], \tag{17}$$

where J is the nearest-neighbor coupling and a denotes the lattice spacing. The latter will be put equal to 1 in all numerical calculations.

III. NONPERTURBATIVE RG

The central idea of the nonperturbative renormalization-group approach to equilibrium condensed-matter systems is to recast the problem of computing the partition function $\mathcal{Z}$ in a form of a (functional) differential equation. There exists a number of variants of this program. The presently applied formulation, developed by Wetterich [44], relies on the concept of a flowing scale-dependent effective action $\Gamma_k[\vec{\phi}]$. This quantity continuously connects the microscopic action [in the present work given by Eq. (11)] with the full free energy F upon varying the flow parameter k. The latter is taken here to be an IR momentum cutoff scale. It serves to add a mass of the order of $\sim k^2$ to the fluctuation modes, effectively freezing their propagation for momenta $q < k$. Lowering the cutoff scale implies including modes of progressively lower momenta. For vanishing k, all fluctuation modes are included into the partition function and we find $\Gamma_k[\vec{\phi}] \longrightarrow \beta F[\vec{\phi}]$ as $k \to 0$. The variation of $\Gamma_k[\vec{\phi}]$ upon changing k is governed by the flow equation [44],

$$\partial_k \Gamma_k[\vec{\phi}] = \tfrac{1}{2}\mathrm{Tr}\big\{\partial_k R_k\big(\Gamma_k^{(2)}[\vec{\phi}] + R_k\big)^{-1}\big\}, \tag{18}$$

where $\Gamma_k^{(2)}[\vec{\phi}]$ denotes the second functional derivative of $\Gamma_k[\vec{\phi}]$. In Fourier space, the trace (Tr) sums over momenta and the field index $a \in \{1,2\}$. The quantity $R_k(q)$ is the momentum cutoff function added to the inverse propagator to freeze the fluctuations with momenta $q < k$. An exact solution of Eq. (18) with the initial condition given by Eq. (11) would imply finding the partition function $\mathcal{Z}$. This is not achievable, but the framework of Eq. (18) offers a number of approximation schemes [26,45–48] going beyond those accessible within the more traditional approaches.

A. Derivative expansion

In this work, we apply the derivative expansion (DE) [45,46,48–50] in which the symmetry-allowed terms in Γ_k are classified according to the number of derivatives (or powers of $\vec{q}$ in momentum space). The most general expression at level ∂^2 (or q^2) reads

$$\Gamma_k[\vec{\phi}] = \int d^2x\big\{U_k(\rho) + \tfrac{1}{2}Z_k(\rho)(\nabla\vec{\phi})^2 + \tfrac{1}{4}Y_k(\rho)(\nabla\rho)^2\big\}, \tag{19}$$

where $\rho = \frac{1}{2}\vec{\phi}^2$. We impose restrictions neither on the effective potential $U_k(\rho)$ nor the gradient functions $Z_k(\rho)$, $Y_k(\rho)$, which are allowed to depend on the cutoff scale k. The occurrence of two gradient terms is due to the fact that the transverse and radial components of the field are characterized by different stiffness coefficients. We also observe here that the initial condition given by Eq. (11) contains terms of all powers of ρ. In fact, the initial condition does not quite fit the ansatz of Eq. (19) since the kinetic term involves functions of arbitrarily high order in $|\vec{q}|$. We come back to this point later on. Plugging the ansatz of Eq. (19) into Eq. (18) yields a projection of the Wetterich equation onto a set of three coupled nonlinear partial differential equations describing the flow of $U_k(\rho)$, $Z_k(\rho)$, and $Y_k(\rho)$, which may be handled numerically. It is advantageous to perform a canonical rescaling of the flowing quantities by defining

$$\tilde{U}_k(\tilde{\rho}) = v_2^{-1}k^{-2}U_k(\rho), \quad \tilde{Z}_k(\tilde{\rho}) = Z_k^{-1}Z_k(\rho),$$
$$\tilde{Y}_k(\tilde{\rho}) = v_2 Z_k^{-2}Y_k(\rho), \tag{20}$$

where $\tilde{\rho} = v_2^{-1}Z_k\rho$ and the factor $v_2^{-1} = 8\pi$ is conventional. The k-dependent constant Z_k (wave-function renormalization) is defined by imposing the condition $\tilde{Z}_k(\tilde{\rho}_\mathrm{r}) = 1$, where $\tilde{\rho}_\mathrm{r}$ is an arbitrary renormalization point on the rescaled grid. The scale-dependent anomalous dimension η is then given by

$$\eta_k = -k\partial_k \ln Z_k, \tag{21}$$

and the physical anomalous dimension follows from $\eta = \lim_{k\to 0}\eta_k$. In a practical calculation, one chooses $\tilde{\rho}_\mathrm{r}$ close to zero, which allows for evading the singularity of the flow described in Ref. [17].

We refrain from quoting the lengthy explicit expressions for the flow equations. These are given in Ref. [16] and in the appendix of Ref. [17]. The transition temperature T_{KT} is extracted following Ref. [17] by using the fact that the flowing minimum $\rho_{0,k}$ of the (nonrescaled) effective potential vanishes as $\rho_{0,k} \sim k^\eta$ in the low-T phase. This is consistent with both the absence of the long-range order and algebraic decay of correlations governed by the anomalous dimension η. Since $Z_k \sim k^{-\eta}$ for $T < T_{KT}$, the minimum of the rescaled potential $\tilde{\rho}_{0,k} = v_2^{-1}Z_k\rho_{0,k}$ remains finite for $k \to 0$ as long as $T < T_{KT}$, and vanishes otherwise.

We also note that a simplified treatment of the present problem [often referred to as the local potential approximation prime (LPA′)], amounting to disregarding the ρ dependencies in the Z factors and projecting the flowing functions $Z_k(\rho)$ and $Y_k(\rho)$ onto scale-dependent constants $Z_k = Z_k(\rho_{0,k})$ and $Y_k = Y_k(\rho_{0,k})$, is not sufficient to capture the KT physics in the vicinity of the transition. The LPA′ truncation suffers from the singularity problem described in detail in Ref. [17]. At the

full derivative expansion level, the problem is circumvented by choosing the renormalization point sufficiently close to zero on the rescaled ρ grid. A procedure of taking the renormalization point at the flowing minimum of the potential leads to an unavoidable singularity of the flow at a finite scale k. The same applies to the LPA′ truncation. We emphasize that this is not an issue of numerical accuracy, but rather an intrinsic property of the flow equations at this truncation level. We also observe that the full derivative expansion generically leads to significantly more accurate numerical estimates of physical quantities [for example, the critical exponents of $O(N)$ models] as compared to LPA′-type treatments.

B. Initial condition for the propagator

The proposed approach relies on two approximations. First, the flowing effective action $\Gamma_k[\vec{\phi}]$ is parametrized by the ansatz of Eq. (19). This implies retaining the most general $U(1)$-invariant form of the action but only up to terms of the order of ∂^2. In particular, the local potential is allowed to contain arbitrarily high powers of ρ. Second, as we already remarked, the initial action of Eq. (11) involves terms of higher order in $|\vec{q}|$ than $|\vec{q}|^2$. We, however, cast it in a form consistent with Eq. (19) by expanding the dispersion in Eq. (11) around $\vec{q}=0$. Physically, this may be understood as "smearing" or coarse graining the lattice structure "by hand." In a somewhat more subtle treatment [35], one might split the flow into two stages. In the initial part ($k > a^{-1}$) of the flow, hardly any renormalization of $Z_k(\rho)$ and $Y_k(\rho)$ occurs, but the cosine dispersion may play a role. One may therefore keep $Z_k(\rho)$ and $Y_k(\rho)$ not renormalized, but include the cosine dispersion inherited from the lattice in the flow equation for $U_k(\rho)$. In the second stage ($k < a^{-1}$), the lattice no longer matters and we may expand all of the inverse propagators in q. Of course, the flow of $Z_k(\rho)$ and $Y_k(\rho)$ must be included for $k < a^{-1}$.

An interesting alternative is provided by the lattice nonperturbative RG framework [35], where the initial stage of the flow is overall bypassed, and the initial condition is not given by the bare action, but, instead, is computed from the local limit of decoupled sites. This program, however, places restrictions on the cutoff, which are most naturally fulfilled by a nonsmooth Litim-type regulator [51]. This in turn renders the flow much less stable numerically. Such complications are most severe in $d=2$. We observe no signatures of numerical instabilities in our variant of approximation. In addition, our calculation requires a significantly smaller field grid than that of Ref. [35].

Our strategy to perform the q expansion from the outset instead of the slightly more accurate treatments mentioned above also stems from the aim to develop a numerically modest and stable framework flexibly extendable to other contexts (such as interacting quantum gases in $d=2$). The present approximation allows one to avoid any two-dimensional integrations in the flow equations. Also observe that the dominant contributions to all of the integrals come from small momenta also for large k, and, of course, upon reducing k the approximation becomes progressively more accurate. By reasoning *a posteriori*, our results suggest that the error from neglecting the cosine dispersion amounts to a shift of the critical temperature (see Sec. IV).

The second derivative matrix in the propagator at the beginning of the flow thus reads

$$\frac{\delta^2 \beta S[\vec{\phi}]}{\delta\phi^{\alpha_1}_{\vec{q}_1}\delta\phi^{\alpha_2}_{\vec{q}_2}} = \delta_{\alpha_1,\alpha_2}\delta_{\vec{q}_1+\vec{q}_2,0}\tilde{A}^{-1}_{\vec{q}_1}. \tag{22}$$

We extract $Z_{k=k_0}(\rho)$ and $Y_{k=k_0}(\rho)$ from the $\vec{q}_1{}^2$ coefficients of the expansion of $\tilde{A}^{-1}_{\vec{q}_1}$ around $\vec{q}_1=0$. Here, $k_0 \gg a^{-1}$ is the initial cutoff scale. In fact, we obtain $Y_{k=k_0}(\rho)=0$ and $Z_{k=k_0}(\rho)=\text{const}>0$. We note that alternative to Eq. (9) ways of rescaling the fluctuating field and interaction matrix, such as that of Ref. [43], generate both $Z_{k=k_0}(\rho)$ and $Y_{k=k_0}(\rho)$ dependencies in the initial condition.

The momentum integrations in the flow equations are computed over a disk of radius $k_{UV}=\pi/a$. In a nonapproximate treatment, they should run over the Brillouin zone ($]-\frac{\pi}{a},\frac{\pi}{a}]\times]-\frac{\pi}{a},\frac{\pi}{a}]$ for a square lattice). The scale k_{UV} is often identified with the scale k_0 where the flow is initiated. In fact, these quantities are distinct, and, in principle, k_0 should be taken infinite to assure that all fluctuations are frozen, so that the action given by Eq. (11) is the correct starting point. In a practical numerical implementation, we take $k_{UV} \ll k_0 < \infty$ and assure that the inverse propagators at high scales are completely dominated by the cutoff term.

C. Numerical solution

Numerical integration of the flow equations proceeds along the lines of Ref. [17]. The ρ grid is uniformly discretized and the problem is cast onto a set of coupled ordinary differential equations. The momentum integrals are computed using a standard Simpson rule and the RG-time stepping is performed within the Euler routine. A typical run takes not more than a few hours on a standard PC machine. For an interesting alternative approach to solving similar systems, we refer to [52,53].

As compared to Ref. [17], there are, however, two important differences. Reference [17] used an effective ϕ^4 action as a starting point, while here the initial condition follows from Eq. (11) (see below). The other difference is that in the present calculation, we extract thermodynamic quantities (specific heat in particular) related directly to the free energy, which is given by $U_{k\to 0}(\rho)$. While for the purposes of Ref. [17] it was sufficient to compute the flow of the $\tilde{\rho}$ derivative of the rescaled potential $\tilde{U}'_k(\tilde{\rho})$, here we additionally compute the flow of the (nonrescaled) potential $U_k(\tilde{\rho})$. The corresponding flow equation, supplementing the flow equations given in Ref. [17], reads

$$\begin{aligned} k^{-1}\partial_k U(\tilde{\rho}) &= \tilde{\rho}\eta\tilde{U}'_k(\tilde{\rho}) \\ &\quad - \int dx[\eta x r(x) + 2x^2 r'(x)] \\ &\quad \times [\tilde{G}_L(x,\tilde{\rho}) + \tilde{G}_T(x,\tilde{\rho})], \end{aligned} \tag{23}$$

where $x = q^2/k^2$ and the dimensionless $\tilde{\rho}$-dependent longitudinal and transverse inverse propagators are given by

$$\begin{aligned} \tilde{G}^{-1}_{\mathrm{L}}(x,\tilde{\rho}) &= x[\tilde{Z}_k(\tilde{\rho}) + \tilde{\rho}\tilde{Y}_k(\tilde{\rho}) + r(x)] + \tilde{U}'_k(\tilde{\rho}) + 2\tilde{\rho}\tilde{U}''_k(\tilde{\rho}), \\ \tilde{G}^{-1}_{\mathrm{T}}(x,\tilde{\rho}) &= x[\tilde{Z}_k(\tilde{\rho}) + r(x)] + \tilde{U}'_k(\tilde{\rho}). \end{aligned} \tag{24}$$

Equation (23) is obtained by first evaluating the Wetterich equation [Eq. (18)] on a uniform field configuration, which yields the flow of the effective potential $U_k(\rho)$ (see, e.g., [46]). Rescaling the ρ grid and changing the integration variable from q to $x = q^2/k^2$ leads to Eq. (23).

A reliable calculation demands high numerical accuracy. This is because we solve the flow equations for a set of initial conditions parametrized by temperature T and subsequently evaluate the entropy and the specific heat by numerically computing the first two derivatives of the result for the free energy with respect to T.

In the practical numerical solution, we employ the smooth Wetterich cutoff,

$$R_k(\vec{q}) = Z_k \vec{q}^2 r(\vec{q}^2/k^2), \quad r(x) = \frac{\alpha}{e^x - 1}. \tag{25}$$

The inclusion of the wave-function renormalization in $R_k(\vec{q})$ is a requirement for the possibility of obtaining scale-invariant solutions. The parameter α is, in principle, arbitrary. Reference [17] posed the question of the existence of exact (functional) fixed points of the flow depending on its value. The present analysis is performed at fixed $\alpha = 2.0$, which is close to the "optimal" value in the immediate vicinity of the transition. We refer to [17] for an extensive discussion of this issue, in particular for the details of the optimization procedure. In fact, the flow singularity problem discussed in Ref. [17] places restrictions on the allowed values of α. Varying α within an admissible range of values changes the position of the transition by a few percent.

IV. NUMERICAL RESULTS

For the nearest-neighbor XY model, $J_{\vec{q}}$ is given by Eq. (17) and it follows that the initial condition for $Z_k(\rho)$ and $Y_k(\rho)$ reads

$$Z_{k_0}(\rho) = Z_0 = \frac{Ja^2}{(c+4J)^2}, \quad Y_{k_0}(\rho) = 0, \tag{26}$$

while the initial effective potential is given by

$$U_{k_0}(\rho) = U_0(\rho) = \frac{1}{(c+4J)}\rho - \log I_0(\sqrt{2\rho\beta}). \tag{27}$$

We observe that both $U_0(\rho)$ and Z_0 depend on the arbitrary parameter c. In fact, as we already pointed out, the mean-field transition temperature of Eq. (16) carries a strong c dependence. Adding fluctuations by the nonperturbative RG flow drastically reduces this dependence, but does not remove it completely, as discussed below. Also observe that (at least formally) the above expressions for $U_0(\rho)$ and $Z_0(\rho)$ make sense for arbitrary non-negative values of c. On the other hand, for the present case of nearest-neighbor interactions, the matrix $\mathbb{A}$ is positive definite for $c > 4$.

A. Critical temperature

The critical temperature T_{KT} is estimated by following the flow of the minimum of the (rescaled) effective potential. This quantity reaches zero at a finite scale $k > 0$ for the system in the high-T phase, and attains an (approximate) fixed point in the KT phase. Equivalently, one may inspect the evolution of the anomalous exponent η_k, vanishing in the high-T phase for k sufficiently small and attaining a "plateau" otherwise. The procedure follows Ref. [17] and is illustrated in Fig. 1, where we plot $\tilde{U}'(0)$ as a function of $s = -\log(k/k_0)$. Also note that the method of estimating T_{KT} is different from the MC, which typically employs a fit of the theoretical formulas for the correlation length and susceptibility to the simulation data. In Ref. [35], only a very weak dependence of the critical temperature on the parameter c was found in the case of the Ising model in three dimensions. In the present case, we observe a monotonous dependence of the KT temperature on the parameter c ranging between $0.91J/k_B$ for $c = 4$ and $1.02J/k_B$ for $c = 8$. The dependence of T_{KT} on c slowly ceases at larger values of c. Large values of c are, however, very unpractical because $Z_0 \sim c^{-2}$ becomes very small. Our estimate of T_{KT} may be compared to the MC results, which give $T_{KT} \approx 0.89J/k_B$. The lattice version of nonperturbative RG yielded the estimate $0.9 < T_{KT}/J < 1$ [35].

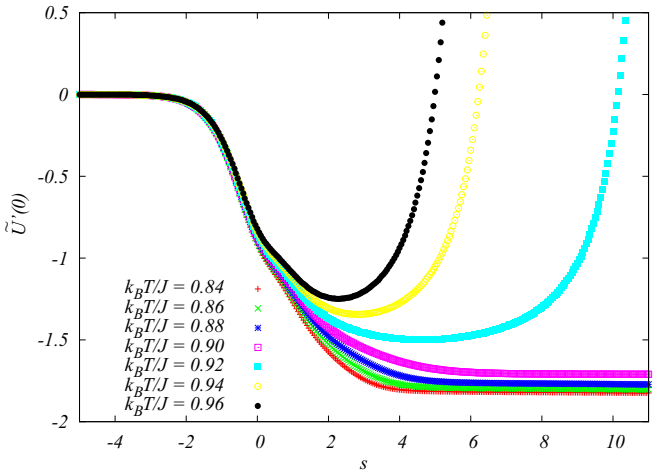

FIG. 1. Exemplary flows of the (rescaled) derivative of the effective potential at $\tilde{\rho} = 0$ for a range of temperatures containing T_{KT} and for $c = 4$. For $T > T_{KT}$, the minimum of the rescaled potential ($\tilde{\rho}_0$) hits zero at a finite scale k, and $\tilde{U}'(0) > 0$. On the other hand, for $T \leqslant T_{KT}$, the flowing couplings [including $\tilde{U}'(0)$] attain fixed-point-like behavior.

We believe that the mechanism responsible for the annihilation (or significant reduction) of the c dependence of the critical temperature is related to the fact that even though the position of the minimum of $U_0(\rho)$ carries a strong c dependence, the minimum $\tilde{\rho}_0$ of the initial rescaled potential $\tilde{U}_0(\tilde{\rho})$ shows only a very weak sensitivity to the variation of c. On the other hand, the profile of $\tilde{U}_0(\tilde{\rho})$ for $\tilde{\rho} < \tilde{\rho}_0$ does depend on c. The dependence of T_{KT} on c should be efficiently eliminated by the flow in situations where the essential features of the flow are captured by the behavior of the effective action around $\tilde{\rho} = \tilde{\rho}_0$. The mechanism is expected to be less efficient otherwise. This condition is better fulfilled in $d = 3$. Our procedure of performing the q expansion from the beginning is also of relevance for the results for T_{KT}. The dependence of our estimate of T_{KT} on c is an unpleasant feature and we perceive it as a deficiency of the present approach. It is possible to choose c so that we obtain T_{KT} in precise agreement with MC, but this is not what we aim for. We note, however, that the c dependence of T_{KT} is by far weaker than at the mean-field

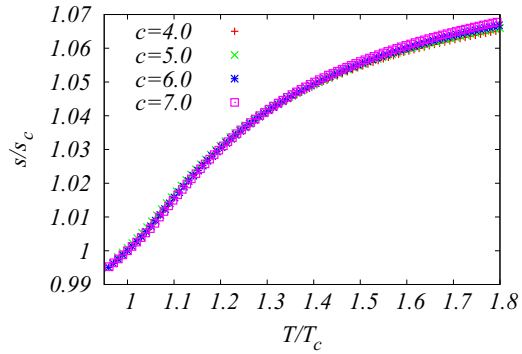

FIG. 2. Entropy as a function of the reduced temperature for a sequence of values of c. The curves collapse once scaled by the critical temperature $T_c = T_{KT}$ and the corresponding entropy density s_c.

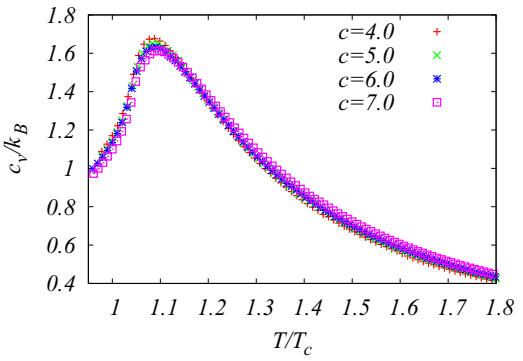

FIG. 3. Specific heat as a function of the reduced temperature for a sequence of values of c. The location and magnitude of the peak agree well with MC and tensor RG (see the main text).

level. In addition, the thermodynamic quantities discussed below are insensitive to the choice of c provided they are computed relative to T_{KT}. This suggests that the error related to our approximation is absorbed by a shift of T_{KT}, leaving other thermodynamic quantities hardly affected.

B. Entropy and specific heat

We proceed by evaluating the entropy at zero magnetic moment (or, equivalently, zero magnetic field), which, by elementary thermodynamics follows from $S(T,N) = Ns(T) = -\frac{\partial F}{\partial T}$. The free energy $F(T,\phi = 0,N)$ is obtained from the integrated flow via $F = k_B T \lim_{k\to 0} U_k(0)$. It is also possible to extend the analysis to nonzero fields since the magnetic field, the order parameter field, and free energy are related by $h = k_B T \lim_{k\to 0} \partial_{|\phi|} U_k(|\phi|)$. By computing the flow for different T, we extract the free-energy profiles $U(\rho)$ for a range of temperatures and subsequently evaluate the (discrete) derivative with respect to T. The results are shown in Fig. 2. We observe a collapse of the curves computed for different c if the variables are scaled by the critical values. The entropy is a positive, monotonously increasing function of temperature, as expected from the principles of thermodynamics. The signatures of the transition are not visible in the T derivatives of the thermodynamic potential (as is expected from the KT theory and also consistent with the results of simulations).

In the next step, we evaluate the specific heat (at zero magnetization). This is given by

$$c_v = T\frac{\partial s}{\partial T} = -\frac{T}{N}\frac{\partial^2 F}{\partial T^2}. \tag{28}$$

The results obtained for different choices of c are plotted in Fig. 3. Again, the dependence on c does not occur once we use the reduced variable. The pronounced maximum shows an asymmetry similar to those found in MC. The peak is located around $T_p \approx 1.1 T_{KT}$ and reaches up to $c_v^m \approx 1.6 k_B$. Both of these quantities are close to the MC and tensor RG results. More specifically (see, e.g., [18,23,25]), the MC peak is located at $T_p^{MC} \approx 1.15 T_c$ and reaches up to $c_v^{m(MC)} \approx 1.5 k_B$. The level of agreement of T_{KT} and c_v between the different Monte Carlo studies [23,25] and the results of tensor RG [25] is very high. However, the entropy is negative at least for some temperatures in both studies. The reason for this is not clear to us.

It is striking that the rich thermodynamic structure described in this section emerged via the functional RG flow from the mean-field free energy, which is trivially equal to zero in the high-T phase (see Sec. II A).

C. Equation of state

The magnetic field $\vec{h}$ at given $\vec{\phi}$ is extracted from the definition

$$\vec{h} = \frac{\partial F}{\partial \vec{\phi}} = k_B T \lim_{k\to 0} \frac{\partial U_k(\rho)}{\partial \vec{\phi}}, \tag{29}$$

which yields the equation of state $\vec{h}(T,\vec{\phi})$. The isothermal susceptibility at zero field is given as the derivative,

$$\chi^{-1}(T) = \frac{\partial h}{\partial \phi}|_{\phi=0} = k_B T v_2^{-1} \lim_{k\to 0}\left[Z_k \frac{\partial U_k(\tilde{\rho})}{\partial \tilde{\rho}}\right]|_{\tilde{\rho}=0}, \tag{30}$$

and becomes very large upon lowering temperature towards T_{KT}. The dependence $\phi(h)$ is shown in Fig. 4 for a sequence of temperatures.

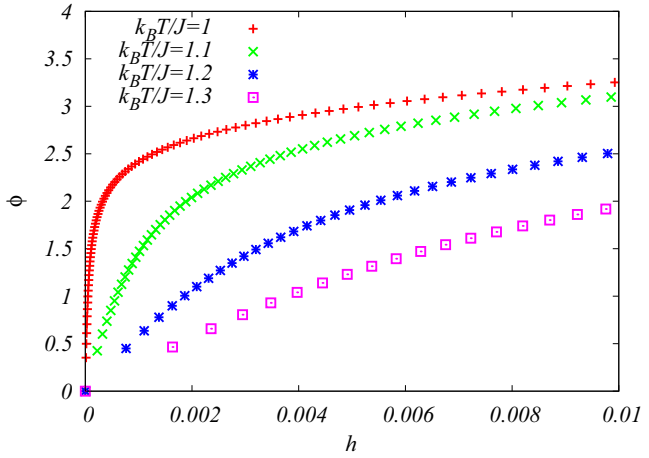

FIG. 4. Dependence of the order parameter on the magnetic field for a sequence of temperatures. The presented calculation was performed at $c = 4$.

V. REMARKS ON THE ϕ^4 TRUNCATION

It is useful to compare the above calculation to a much simpler treatment relying on the ϕ^4-type expansion. It is natural to invoke a largely simplified ansatz for the effective potential,

$$U_k(\rho) = \frac{\lambda_k}{2}(\rho - \rho_{0,k})^2 + \gamma_k, \tag{31}$$

and also restrict $Z_k(\rho)$ and $Y_k(\rho)$ to flowing couplings corresponding to the functions evaluated at the potential minimum (ρ_0). The problem may then be cast onto a set of five coupled ordinary differential flow equations for the couplings $\rho_{0,k}$, λ_k, γ_k, Z_k, and Y_k. The initial condition for the potential is extracted by expanding the effective potential in Eq. (11) around its minimum. The ansatz given by Eq. (31) makes sense for $Z_k\rho_{0,k} > 0$. Once the flow crosses over into the regime with $Z_k\rho_{0,k} = 0$, one switches to the parametrization suitable for the high-temperature phase,

$$U_k(\rho) = \frac{\lambda_k}{2}\rho^2 + \delta_k\rho + \gamma_k. \tag{32}$$

The free energy may then be extracted from $\lim_{k\to 0}\gamma_k$. In fact, a very similar truncation (neglecting Y_k and γ_k) was employed in Ref. [15] and yielded a plausible picture of the KT transition.

We have solved the above-mentioned set of flow equations and compared the results to those obtained within the complete derivative expansion in Sec. IV. Even though the estimate of the critical temperature T_{KT} is in a reasonable range, the ϕ^4 approximation badly fails for the thermodynamic quantities. In fact, the obtained free energy $F(T)$ is not a concave function of temperature, yielding, for example, a negative specific heat in a range of temperatures. The reason for this becomes clear after inspecting Eq. (11). Expanding the effective potential in ρ implies uncontrolled dropping of temperature dependencies, which, as it turns out, leads to a drastic deformation of the result.

VI. SUMMARY AND OUTLOOK

We have solved the nonperturbative RG flow equations for the two-dimensional XY model at the approximation level of the complete second-order derivative expansion. From the obtained free energy $F(T,\phi,N)$, we computed the nonuniversal thermodynamic properties in the high-temperature phase. Wherever possible, we compared the results to Monte Carlo simulations. We found satisfactory agreement for the entropy and specific heat. In particular, the location and magnitude of the specific-heat peak relative to T_{KT} compare very well to MC data. This is one of the few RG-based computations for this quantity in this model. As we pointed out, the specific-heat peak occurs in a regime which, on the one hand, is off the asymptotic critical region, and, on the other hand, is characterized by large correlation length. Such a situation is somewhat atypical. An interesting RG calculation was performed in Ref. [25] within the tensor RG framework, which may be viewed as a reincarnation of the ideas of a direct real-space coarse-graining scheme. However, it is not clear to what extent that approach can be generalized to other systems.

Our estimate of the Kosterlitz-Thouless temperature is not far from the correct value; however, the present method cannot serve as a high-precision tool in this case. We argue that the location of the transition is the quantity that is most strongly affected by the approximations, in particular by the relatively simple treatment of the dispersion at the initial stages of the flow. As we pointed out, the thermodynamic functions become insensitive to the arbitrary parameter c of the Hamiltonian upon scaling by T_{KT}.

We compared the full derivative expansion to a simplified treatment invoking vertex expansion (ϕ^4-type theory), which is commonly applied in different contexts. The latter framework turns out not to be sufficient for computing the nonuniversal thermodynamic quantities, since it truncates relevant temperature dependencies in the neglected vertices.

The present calculation bridges a microscopic model with macroscopic thermodynamics via the functional flow equation, accounting for the low-energy asymptotics specific to two-dimensional systems with $U(1)$ symmetry. It will now be natural and interesting to perform analogous studies of systems characterized by similar infrared physics, including interacting quantum gases in $d = 2$.

ACKNOWLEDGMENTS

We are grateful to Bertrand Delamotte, Nicolas Dupuis, and Walter Metzner for useful discussions. We also thank Walter Metzner for reading the manuscript and a number of valuable remarks. P.J. acknowledges funding from the Polish National Science Center via Grant No. 2014/15/B/ST3/02212. A.E. acknowledges support from the German National Academy of Sciences Leopoldina through Grant No. LPDS 2014-13.

[1] V. L. Berezinskii, Sov. Phys. JETP **32**, 493 (1971).
[2] V. L. Berezinskii, Sov. Phys. JETP **34**, 610 (1972).
[3] J. M. Kosterlitz and D. J. Thouless, J. Phys. C **6**, 1181 (1973).
[4] J. M. Kosterlitz and D. J. Thouless, J. Phys. C **7**, 1046 (1974).
[5] J. Fröhlich and T. Spencer, Commun. Math. Phys. **81**, 527 (1981).
[6] N. D. Mermin and H. Wagner, Phys. Rev. Lett. **17**, 1133 (1966).
[7] P. M. Chaikin and T. C. Lubensky, *Principles of Condensed Matter Physics* (Cambridge University Press, Cambridge, 1995).
[8] D. J. Bishop and J. D. Reppy, Phys. Rev. Lett. **40**, 1727 (1978).
[9] J. Maps and R. B. Hallock, Phys. Rev. Lett. **47**, 1533 (1981).
[10] J. Maps and R. B. Hallock, Phys. Rev. B **26**, 3979 (1982).
[11] Z. Hadzibabic, P. Krüger, M. Cheneau, B. Battelier, and J. Dalibard, Nature (London) **441**, 1118 (2006).
[12] S. Tung, G. Lamporesi, D. Lobser, L. Xia, and E. A. Cornell, Phys. Rev. Lett. **105**, 230408 (2010).
[13] R. Desbuquois, L. Chomaz, T. Yefsah, J. Léonart, J. Beugnon, C. Weitenberg, and J. Dalibard, Nat. Phys. **8**, 645 (2012).
[14] P. A. Murthy, I. Boettcher, L. Bayha, M. Holzmann, D. Kedar, M. Neidig, M. G. Ries, A. N. Wenz, G. Zürn, and S. Jochim, Phys. Rev. Lett. **115**, 010401 (2015).
[15] M. Gräter and C. Wetterich, Phys. Rev. Lett. **75**, 378 (1995).

[16] G. v. Gersdorff and C. Weterich, Phys. Rev. B **64**, 054513 (2001).
[17] P. Jakubczyk, N. Dupuis, and B. Delamotte, Phys. Rev. E **90**, 062105 (2014).
[18] J. Tobochnik and G. V. Chester, Phys. Rev. B **20**, 3761 (1979).
[19] J. E. Van Himbergen and S. Chakravarty, Phys. Rev. B **23**, 359 (1981).
[20] P. Olsson, Phys. Rev. B **52**, 4526 (1995).
[21] M. Hasenbusch and K. Pinn, J. Phys. A: Math. Gen. **30**, 63 (1997).
[22] M. Hasenbusch, J. Phys. A: Math. Gen. **38**, 5869 (2005).
[23] J. Xu and H.-R. Ma, Phys. Rev. E **75**, 041115 (2007).
[24] Y. Komura and Y. Okabe, J. Phys. Soc. Jpn. **81**, 113001 (2012).
[25] J. F. Yu, Z. Y. Xie, Y. Meurice, Y. Liu, A. Denbleyker, H. Zou, M. P. Qin, J. Chen, and T. Xiang, Phys. Rev. E **89**, 013308 (2014).
[26] W. Metzner, M. Salmhofer, C. Honerkamp, V. Meden, and K. Schönhammer, Rev. Mod. Phys. **84**, 299 (2012).
[27] S. Friederich, H. C. Krahl, and C. Wetterich, Phys. Rev. B **83**, 155125 (2011).
[28] K.-U. Giering and M. Salmhofer, Phys. Rev. B **86**, 245122 (2012).
[29] A. Eberlein and W. Metzner, Phys. Rev. B **89**, 035126 (2014).
[30] T. Kloss, L. Canet, and N. Wschebor, Phys. Rev. E **86**, 051124 (2012).
[31] T. Kloss, L. Canet, and N. Wschebor, Phys. Rev. E **90**, 062133 (2014).
[32] D. Mesterházy, J. H. Stockemer, and Y. Tanizaki, Phys. Rev. D **92**, 076001 (2015).
[33] F. Léonard and B. Delamotte, Phys. Rev. Lett. **115**, 200601 (2015).
[34] B. Delamotte, M. Tissier, and N. Wschebor, Phys. Rev. E **93**, 012144 (2016).
[35] T. Machado and N. Dupuis, Phys. Rev. E **82**, 041128 (2010).
[36] A. Codello and G. D'Odorico, Phys. Rev. Lett. **110**, 141601 (2013).
[37] H. C. Krahl and C. Wetterich, Phys. Lett. A **367**, 263 (2007).
[38] S. Floerchinger and C. Wetterich, Phys. Rev. A **79**, 013601 (2009).
[39] A. Rançon and N. Dupuis, Phys. Rev. A **85**, 063607 (2012).
[40] A. Rançon and N. Dupuis, Europhys. Lett. **104**, 16002 (2013).
[41] A. Rançon, Phys. Rev. B **89**, 214418 (2014).
[42] P. Strack and P. Jakubczyk, Phys. Rev. X **4**, 021012 (2014).
[43] D. Amit and V. Martin-Mayor, *Field Theory, Renormalization Group, and Critical Phenomena*, 3rd ed. (World Scientific, Singapore, 2005).
[44] C. Wetterich, Phys. Lett. B **301**, 90 (1993).
[45] T. R. Morris and M. D. Turner, Nucl. Phys. B **509**, 637 (1998).
[46] J. Berges, N. Tetradis, and C. Weterich, Phys. Rep. **363**, 223 (2002).
[47] P. Kopietz, L. Bartosch, and F. Schütz, *Introduction to the Functional Renormalization Group* (Springer, New York, 2010).
[48] B. Delamotte in *Renormalization Group and Effective Field Theory Approaches to Many-Body Systems*, Lecture Notes in Physics, Vol. 852, edited by A. Schwenk and J. Polonyi (Springer, New York, 2012).
[49] L. Canet, B. Delamotte, D. Mouhanna, and J. Vidal, Phys. Rev. B **68**, 064421 (2003).
[50] B. Delamotte, D. Mouhanna, and M. Tissier, Phys. Rev. B **69**, 134413 (2004).
[51] D. Litim, Phys. Rev. D **64**, 105007 (2001).
[52] J. Borchardt and B. Knorr, Phys. Rev. D **91**, 105011 (2015).
[53] J. Borchard and B. Knorr, arXiv:1603.06726v1.